

# Evolution of magnetic circular dichroism of pure ZnTe in magnetic field: Spectral similarity between undoped and Cr-doped ZnTe

Hongming Weng,<sup>1,\*</sup> Jinming Dong,<sup>2</sup> Tomoteru Fukumura,<sup>1</sup> Masashi Kawasaki,<sup>1</sup> and Yoshiyuki Kawazoe<sup>1</sup>

<sup>1</sup>*Institute for Materials Research, Tohoku University, 2-1-1 Katahira, Aoba-ku, Sendai 980-8577, Japan*

<sup>2</sup>*Group of Computational Condensed Matter Physics, National Laboratory of Solid State Microstructure and Department of Physics, Nanjing University, Nanjing 210093, People's Republic of China*

(Received 6 November 2007; published 10 March 2008)

Magnetic circular dichroism (MCD) spectra of pure ZnTe in various external magnetic field have been studied with first-principles calculations. By applying magnetic field on undoped semiconductor, the effects of spin splitting in host's bands due to  $s,p-d$  exchange interactions in diluted magnetic semiconductors (DMSs) have been largely simulated. At the same time, the complexity of band structure in DMS is avoided since no magnetic ion is doped, which facilitates the band-to-band analysis of MCD spectra. The obtained MCD spectra of undoped ZnTe within low magnetic field are found to be proportional to the field strength and comparable with the experimental measurements. Within high magnetic field, where the Zeeman splitting is comparable with spin-orbit coupling strength, the MCD spectra become as similar as those of Cr-doped ZnTe around the  $L$  critical points. Thus, the MCD signal contributed by the spin-split bands of host semiconductor is identified and separated from those due to the introduction of Cr  $3d$  or  $4s$  impurity bands. These results indicate that the experimentally observed MCD spectra can be well reproduced and understood by band structure calculations.

DOI: [10.1103/PhysRevB.77.125206](https://doi.org/10.1103/PhysRevB.77.125206)

PACS number(s): 75.50.Pp, 78.20.Ls, 75.30.Et

## I. INTRODUCTION

The essence of diluted magnetic semiconductor (DMS) is the strong  $s,p-d$  exchange interactions between the  $s,p$  carriers of host semiconductor and the local  $d$  electrons of doped magnetic transition-metal ions, which assures the realization of mutual control of magnetic, electric, and optical properties in DMS based spintronic devices. These  $s,p-d$  exchange interactions can induce much larger spin splitting in the conduction and valence bands than external magnetic field might do. As a result, magneto-optical effects in DMS are largely enhanced by several orders compared with those in an undoped semiconductor within external magnetic field. For example, the magnetic circular dichroism (MCD) spectrum, defined as the difference of optical absorption between right- and left-handed circularly polarized light, is largely enhanced in DMS especially around the critical points of host semiconductor.<sup>1</sup> A set of critical points is a fingerprint of one material. Measurement and analysis of MCD spectrum can easily identify what kind of material contributes to the observed signals.<sup>1</sup> According to the definition of MCD, it is suggested that MCD signal is proportional to  $-\Delta E dR/dE$ , where  $\Delta E$  is the difference of the exciting energies between the right- and left-handed circularly polarized light due to spin splitting effect and  $dR/dE$  is the derivative of absorption coefficient  $R$  with photon energy  $E$ . Here,  $\Delta E$  is directly correlated with the magnitude and polarity of spin splitting due to external magnetic field or  $s,p-d$  exchange interactions. Therefore, MCD is naturally proposed as a direct and efficient way to detect and characterize the  $s,p-d$  exchange interactions in DMS.<sup>2</sup> There have been many experimental efforts performed on various DMS systems in order to illustrate the efficiency of MCD method. For example, in GaAs:Mn,<sup>3</sup> GaN:Mn,<sup>4</sup> GaAs:Cr,<sup>5</sup> InAs:Mn,<sup>6</sup> ZnTe:Cr,<sup>7</sup> and ZnO:Co,<sup>8,9</sup> the existence and the polarity of  $s,p-d$  exchange interactions have been confirmed and clarified. These sys-

tems are convinced to be real DMSs. In addition, further MCD analysis clarified that only GaAs:Mn, InAs:Mn, and ZnTe:Cr are intrinsic ferromagnetism (FM) DMSs, while ZnO:TM (TM=Mn, Fe, Co, Ni, or Cu), GaN:Mn, and GaAs:Cr are paramagnetic DMSs and the observed FM behaviors in them may come from some unknown precipitations that have not been detected by crystallographic studies.<sup>2,9</sup>

Despite these intensive experimental efforts, up to now, a theoretically well-established correlation between the shape of MCD and the underlying band structure has not been demonstrated or studied.<sup>2</sup> Theoretical studies, especially *ab initio* calculations of MCD spectrum in DMS, are still very few although they are urgently needed for identifying the experimentally observed MCD signals and justifying the capability of this method in estimation of  $s,p-d$  exchange interactions. For this purpose, accurate studies of MCD spectra by band structure calculations had been performed by us on two systems: the Co-doped TiO<sub>2</sub> (Ref. 10) and Cr-doped ZnTe (Zn<sub>1-x</sub>Cr<sub>x</sub>Te) DMSs.<sup>11</sup> Both of them have been reported to have room-temperature ferromagnetism and seem to be promising for applications in spintronic devices. The former represents the newly discovered oxide DMSs, while the later is the prototype of classical II-VI semiconductor DMS within zinc-blende (ZB) structure. Further detailed studies of this prototype DMS would be greatly helpful to the understanding of all the DMS systems.

To demonstrate or establish the connection between observed physical property, such as MCD spectra treated here, and underlying band structure, the state-of-the-art and parameter free first-principles calculation based on density functional theory is a natural and effective method. In DMS, the band structure is quite complex due to the impurity bands of sparsely doped transition metals and the band folding effect introduced by supercell technique used for simulating the low doping concentration. Detailed band-to-band analy-

sis of the contributions to MCD signal and its shape is neither easy nor direct. On the other hand, since the doping concentration is quite low, most of the model understandings or explanations of MCD are generally based on the spin-split band structure of undoped host semiconductors due to the  $s, p$ - $d$  exchange interaction.<sup>1</sup> The band structure of undoped semiconductor with ZB structure is very simple and well studied, and it has been shown to have advantages in understanding the magneto-optical Kerr effects in ZB transition-metal chalcogenides by band-to-band analysis.<sup>12</sup> From the point of view of magneto-optical responses, the most important difference between DMS and undoped host semiconductor is whether there is spin splitting in the energy bands or not. One of the simplest ways to mimic this profound effect due to  $s, p$ - $d$  exchange interactions in DMS is to apply external magnetic field onto the pure host semiconductors. By doing this, the impurity bands and the band folding effect will be able to totally avoided, while the spin splitting effect can be largely simulated. Therefore, the MCD spectra of pure host semiconductors within external magnetic field and the corresponding DMS are expected to have some similarities. If there were, these similar MCD structures could be called intrinsic contributions since they come from the host's spin-split  $s$  and  $p$  bands. The differences between them are naturally ascribed to the contributions due to the transitions from or to these impurity bands, which, accordingly, are called extrinsic contributions.

In this paper, we will perform the MCD spectra calculations for pure ZnTe within different strengths of magnetic field and compare them with those of Cr-doped ZnTe DMSs ( $\text{Zn}_{1-x}\text{Cr}_x\text{Te}$ ) in order to present a good understanding of MCD spectra in DMS from the viewpoint of band structure. In the next section, we will briefly introduce our calculation method. The results as well as discussions of them are presented in Sec. III. Finally, a brief summary is made in Sec. IV.

## II. METHODOLOGY

The highly accurate all electron full-potential linearized augmented plane-wave method implemented in WIEN2K<sup>13</sup> is used for electronic structure calculation within the generalized gradient approximation (GGA).<sup>14</sup> In  $\text{Zn}_{1-x}\text{Cr}_x\text{Te}$ , to simulate the doping concentration of  $x=0.0625$  and  $0.25$ , one apical Zn atom is replaced by Cr in a  $\sqrt{2} \times \sqrt{2} \times 2$  and  $1 \times 1 \times 1$  supercells of the ZB ZnTe, respectively. The spin-orbit coupling (SOC) is taken into account with the magnetization aligned along the [001] directions by using the second-variation method<sup>15</sup> self-consistently. In pure ZnTe, the interaction with external magnetic field is taken into account self-consistently by adding an additional potential  $V_{B_{ext}}^- = \mu_B \vec{B}_{ext} \cdot (\vec{l} + 2\vec{s})$ , where  $\vec{B}_{ext}$  is the external magnetic field strength, while  $\vec{l}$  and  $\vec{s}$  are the orbital and spin moment of the corresponding electrons, respectively. The direction of  $\vec{B}_{ext}$  is along [001], too. Obviously, the Landau quantization and diamagnetic shifting effects in semiconductor caused by external magnetic field are neglected here. Such a kind of simplification is suitable for simulating the effect of the  $s, p$ - $d$

exchange interactions in DMSs since they cause only spin splitting in host semiconductor bands without the Landau quantization nor diamagnetic shifting effects.

The optical conductivity tensor  $\sigma_{\alpha\beta}$  ( $\alpha, \beta \equiv x, y, z$ ) is calculated within the electric-dipole approximation using the well-known Kubo linear-response formula,<sup>12,16</sup>

$$\sigma_{\alpha\beta}(\omega) = \frac{ie^2}{m^2 \hbar V} \sum_k \sum_{j,j'} \frac{f(E_{jk}) - f(E_{j'k})}{\omega_{jj'}} \left[ \frac{\Pi_{j'j}^\alpha \Pi_{jj'}^\beta}{\omega - \omega_{jj'} + i/\tau} + \frac{(\Pi_{j'j}^\alpha \Pi_{jj'}^\beta)^*}{\omega + \omega_{jj'} + i/\tau} \right]. \quad (1)$$

Here,  $f(E_{jk})$  is the Fermi function,  $\hbar\omega_{jj'} = E_{jk} - E_{j'k}$  is the energy difference of the Kohn-Sham energies  $E_{jk}$ , and  $\tau^{-1}$  is the inverse of the lifetime of excited Bloch electron states, the only parameter used in the whole calculation. A value of  $\hbar/\tau = 0.1$  eV is adopted in this paper if not specified. Here,  $\Pi_{j'j}^\alpha$  is the element of the dipole optical transition matrix. The upper limit of the band indices  $j$  and  $j'$  is taken as the band lying at as high as 2.5 Ry above Fermi level, and the convergence is carefully checked by varying it from 1.5 to 3.5 Ry. The convergence for the integral of  $k$  space is also tested. Once the elements of the optical conductivity tensor are obtained, the right- ( $\alpha^+$ ) and left-handed ( $\alpha^-$ ) circularly polarized light absorption are calculated by  $\alpha^\pm \approx 4\pi \text{Re}(\sigma_{xx} \pm i\sigma_{xy})c$ , with  $c$  as the speed of light.<sup>17</sup>

## III. RESULT AND DISCUSSION

The Zeeman splitting has a small effect. An external magnetic field as strong as 10 or 50 T has no obvious effects on the band structure and absorption spectrum of ZnTe, as shown in Fig. 1. All of them are nearly superposed. A set of critical points is indicated by  $E_0$ ,  $E_1$ , and  $E_1 + \Delta_1$ . Arrows in Fig. 1(a) denote that the absorption edge is contributed by the direct band gap transition at  $\Gamma$  point and the two  $L$ -critical points (CPs),  $E_1$  and  $E_1 + \Delta_1$ , come from the transitions at  $L$  point, where SOC lifts the degeneracy of light and heavy hole bands by a gap of  $\Delta_1$ . All of the obtained CPs are lower than the experimental values by about 1.2 eV since the band gap is underestimated, which is a well-known shortcoming of GGA.<sup>18</sup> To distinguish the effects of magnetic field clearly, MCD spectra are plotted in Fig. 2. For  $B=0$  T, the MCD signal is nearly none. While for the magnetic field  $B=10$  or 50 T, the calculated MCD signal has noticeable and interesting structures around the absorption CPs. It is noticed that the five times enlarged spectrum of  $B=10$  T is well overlapped with that of  $B=50$  T, which means the MCD signal is proportional to the magnetic field strength. This is consistent with the relationship between MCD and the Zeeman splitting energy  $\Delta E$ . Most importantly, these theoretical MCD spectra within external magnetic field are well comparable with the experimental measurement.<sup>9</sup> The whole shape of the experimental spectrum, especially the characteristic double positive peaks around the two  $L$ -CPs, is well reproduced by our calculations.  $dR/dE$  is plotted together and it also has double positive peaks around  $E_1$  and  $E_1 + \Delta_1$ , which

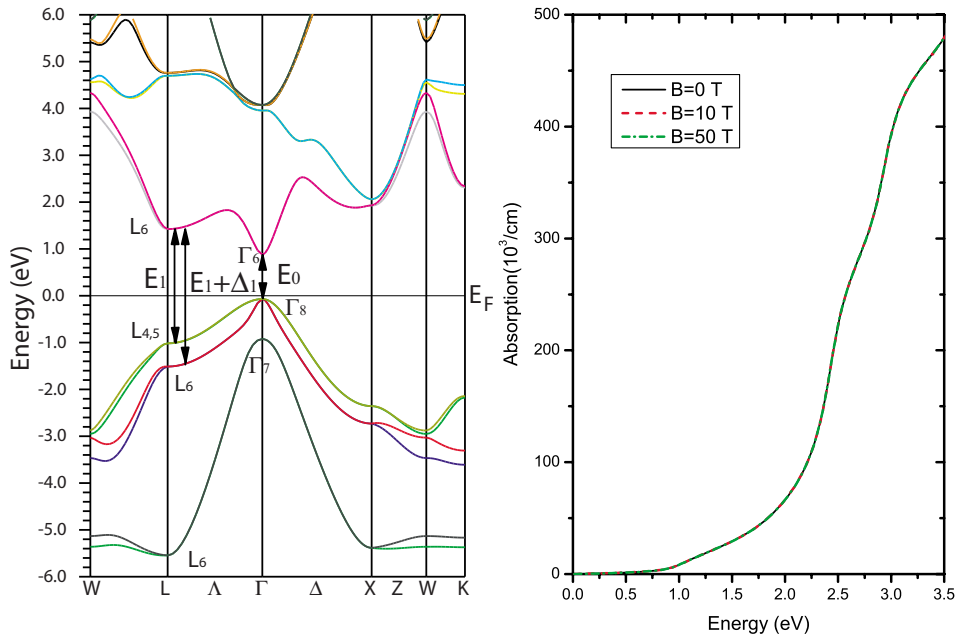


FIG. 1. (Color online) The (a) band structure and (b) absorption spectra of pure ZnTe within different magnetic fields. Arrows denoting the band transitions contribute to  $E_0$ ,  $E_1$ , and  $E_1+\Delta_1$  critical points.

means the Zeeman splitting polarities are the same at these two  $L$ -CPs.

Within mean field approximation, the spin splittings of host's conduction and valence bands in DMS are expressed as  $x\langle S_z \rangle N_0\alpha$  and  $x\langle S_z \rangle N_0\beta$ , respectively.<sup>19,20</sup>  $x\langle S_z \rangle$  is looked as an effective magnetic field with  $x$  being the doping concentration and  $\langle S_z \rangle$  being the local spin on the transition-metal ion.  $N_0\alpha$  and  $N_0\beta$  are the  $s$ - $d$  and  $p$ - $d$  exchange integral parameters, respectively. Since the doping concentration is quite small, such spin splitting could be looked as a perturbation compared to the spin-orbit splitting. Within these interactions, the energy level diagram around  $\Gamma$  is quite simple. First, the SOC splits the sixfold degenerated (counting also the degree of freedom of spin) valence band maximum into the twofold split-off ( $\Gamma_7, p_{1/2}$ ) and fourfold ( $\Gamma_8, p_{3/2}$ ) heavy and light hole substates, as shown in Fig.

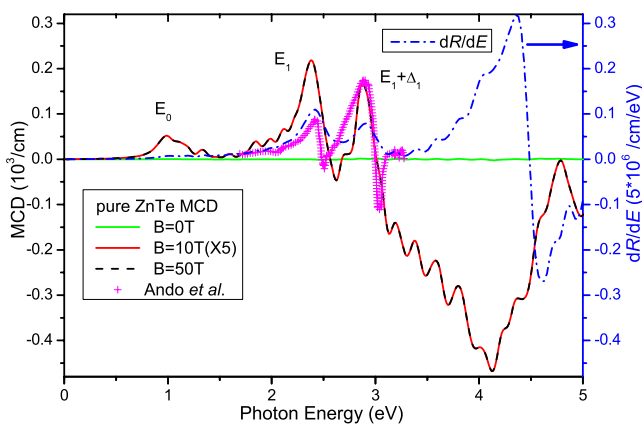


FIG. 2. (Color online) The calculated (lines) and experimental (symbol) MCD spectra for pure ZnTe within different magnetic fields.  $dR/dE$  is also plotted with dash-dotted line. The experimental spectrum taken from Ref. 9 is shifted to lower energy by about 1.2 eV in order to match the theoretical critical points  $E_0$ .

1(a). Then, the  $s, p$ - $d$  exchange interactions act as a perturbation to further remove the remaining degeneracy. The energy order of these bands is critical to the red- or blueshift in the absorption of circularly polarized light due to the selection rule. This picture has been used for describing various magneto-optical effects in Ref. 1 in detail. However, it is well known that  $p$ - $d$  exchange interactions (in the order of eV) are quite larger than or comparable with the strength of SOC (in the order of 0.1 eV or smaller) in most semiconductors. If  $x$  is large enough, the effective spin splitting will be comparable with or even larger than the spin-orbit splitting, then the above energy level diagram will change. As demonstrated in Ref. 21, the mixing of split-off and light hole states becomes larger when the effective spin splitting increases with  $x$ . In this case, the six  $p$  bands are first splitted into two triply degenerated spin up and down groups, and then in each group, SOC further splits the three bands equally. Such picture is clearly shown in Fig. 3(a) in the band structure of hypothetical 100% Cr-doped ZnTe, the ZB CrTe.<sup>12</sup> The spin splitting due to the  $p$ - $d$  exchange interaction between Te 5 $p$  and Cr 3 $d$  is as large as 1.0 eV,<sup>12</sup> larger than the spin-orbit splitting in ZnTe, about 0.85 and 0.5 eV at  $\Gamma$  and  $L$  points, respectively. To simulate such a case in pure ZnTe, we need to apply a quite large magnetic field. A rough estimation based on the Zeeman effect indicates that the spin splitting induced in Te  $p$  bands by a magnetic field as strong as  $B=5000$  T would be comparable with that in CrTe. Within such strong magnetic field, the band structure and optical properties are found to have obvious changes compared to those within low magnetic field. As shown in Fig. 3(b), the Zeeman splitting in each band is quite large and similarities in the Te  $p$  bands are easy to be found when compared with that of CrTe. Obviously, the perturbation picture is not suitable for this case anymore. Such changes in energy levels should bring changes in the absorption and MCD spectra accordingly. In Fig. 4(a), the absorption spectra for  $B=50$  and 5000 T are plotted. As in the usual case, absorption

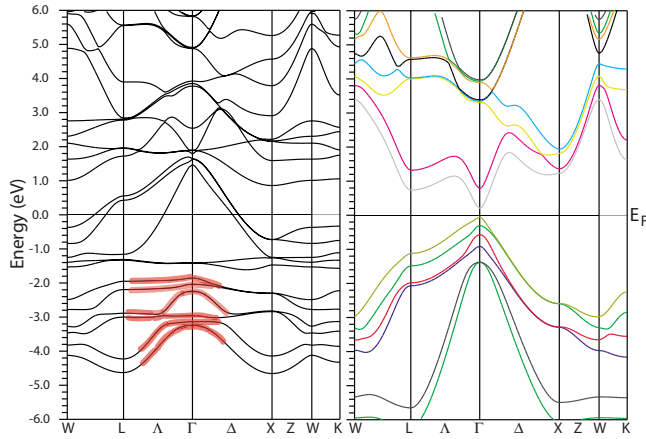


FIG. 3. (Color online) Calculated band structure of (a) hypothetical 100% Cr-doped ZnTe and (b) undoped ZnTe within  $B=5000$  T. In (a), the bands composed of Te  $p$  orbitals are highlighted.

spectra can give very limited information. Noticeable changes can only be seen around the  $E_1$  and  $E_1+\Delta_1$  CPs. While in the MCD spectra, nontrivial changes have been observed. The typical double positive peak structure now changes to be one positive and one negative structure, as shown in Fig. 4(b). Surprisingly, such MCD structure is nearly the same as that in Cr-doped ZnTe DMS.<sup>11</sup> We will discuss this more below.  $dR/dE$  is also plotted in Fig. 4(b). It keeps positive at two  $L$  points, the same as in  $B=50$  T case, which means the polarity of Zeeman splitting at  $E_1+\Delta_1$  now has changed.<sup>22</sup>

Now, we can move to the real DMS system, Cr-doped ZnTe. First, let us examine the band structure for 25% doping case.<sup>11</sup> Comparing its band structure (Fig. 5) with those of ZB CrTe and pure ZnTe within  $B=5000$  T (Fig. 3), we will find some similarities in their band structures, especially in the occupied Te  $p$  and unoccupied Zn  $s$  bands as highlighted in the figures. Transitions between these spin polar-

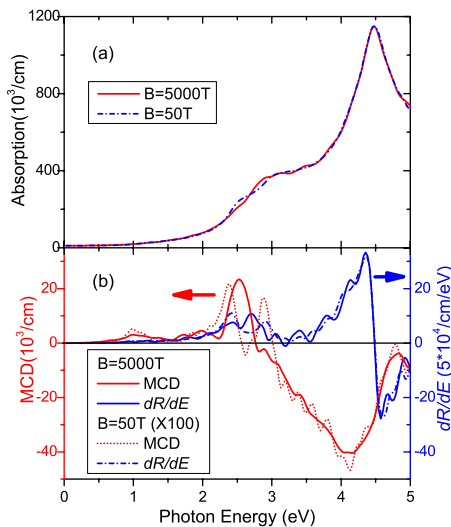


FIG. 4. (Color online) Calculated (a) absorption and (b) MCD spectra for undoped ZnTe within  $B=5000$  and 50 T.

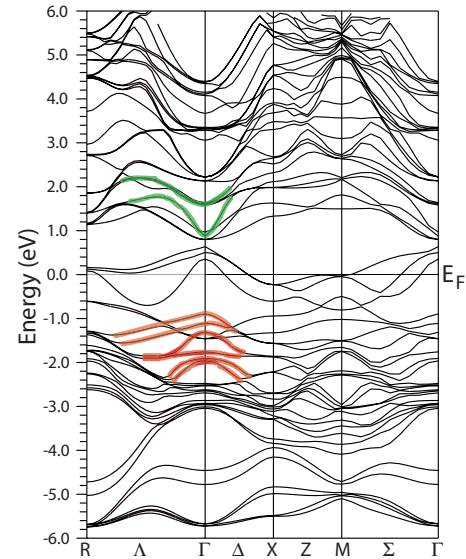


FIG. 5. (Color online) The band structure for 25% Cr-doped ZnTe DMS. The occupied Te  $p$  and unoccupied Zn  $s$  bands are highlighted.

ized bands contribute to the corresponding MCD signals around  $E_1$  and  $E_1+\Delta_1$ . The similar band structures are expected to give rise to the similar MCD spectra. It is true if we compare their MCD spectra in Fig. 6. Obviously, the MCD spectra around  $L$ -CPs are quite consistent with that of pure ZnTe within  $B=5000$  T magnetic field even in some fine details. Interestingly, the experimentally measured MCD spectra of Cr-doped ZnTe samples also have quite similar MCD spectra around the two  $L$ -CPs.<sup>7,23</sup> These indicate that such a kind of MCD structure is common and intrinsic, purely contributed by the polarized band structure of host semiconductor. The differences in these MCD spectra lower than 1.0 eV and around 4.0 eV could be easily ascribed to the introduction of Cr  $3d$  and  $4s$  impurity bands in the doping case. These could be called extrinsic due to impurity bands of Cr. However, the difference in the experimental MCD spectra from two samples, especially those between  $E_0$

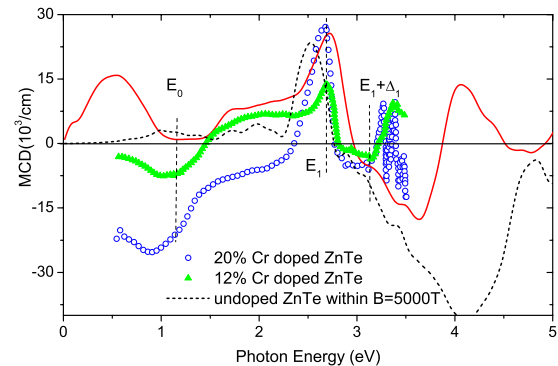


FIG. 6. (Color online) Calculated MCD spectra for 25% Cr-doped ZnTe (solid line) and that of pure ZnTe within magnetic field  $B=5000$  T (dashed line). For comparison, the experimental spectra for 20% (triangle, from Ref. 7) and 12% (circle, from Ref. 23) Cr-doped ZnTe are also plotted.



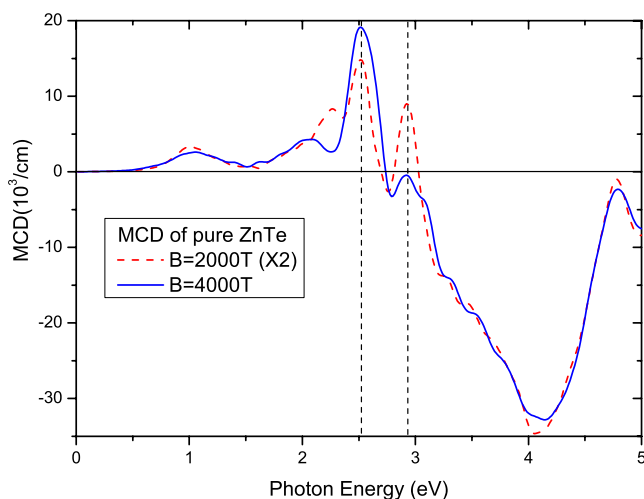


FIG. 7. (Color online) (a) The MCD spectra for pure ZnTe within magnetic field  $B=2000$  T (dashed line) and  $B=4000$  T (solid line).

and  $E_1$  points, may be due to the sample quality difference, such as the different carrier and doping concentrations, which had been discussed in Ref. 11. The difference between theoretical and experimental spectra around  $E_0$  had been related to the lack of carriers in calculations in Ref. 11, too.

As mentioned above, red- or blueshift of the absorption energy for circularly polarized light is determined by the order of angular momentum of corresponding energy bands.<sup>1</sup> Within high magnetic field, spin-split bands with  $j=3/2$  (heavy hole) and  $j=1/2$  (light hole) at  $L$  point would have band crossing if the splitting is larger than the spin-orbit splitting. Such kind of band order change certainly will have direct and nontrivial influence on the corresponding MCD signals. A simple estimation based on the Zeeman effect indicates that the critical magnetic field strength is around 3200 T corresponding to the 0.5 eV spin-orbit splitting at  $L$  point in ZnTe. Magnetic fields larger than this will make the spin-split heavy and light hole bands at  $L$  point cross each other and bring changes in the absorption of circularly polarized light. As shown in Fig. 7, within magnetic field  $B=2000$  T, MCD spectrum of ZnTe still has the double positive peaks structure at the two  $L$ -CPs, while within 4000 T, the second positive signal becomes negative, the same as that within 5000 T fields and also those of  $\text{Zn}_{1-x}\text{Cr}_x\text{Te}$ . Such positive to negative transition is also found in GaAs though

the critical magnetic field strength is smaller, about 1300 T, since the spin-orbit splitting at  $L$  point in GaAs is only around 0.2 eV. Another plausible reason is the Paschen-Back effect. When magnetic field is strong enough and comparable with the SOC strength, spin and orbital moment would be decoupled and the Paschen-Back effect appears, which has different band splitting pattern from that in the weaker magnetic field. It has the same number of spectral lines as the normal Zeeman effect and fewer than that of the anomalous Zeeman effect. There are only one unpolarized light sandwiched by one right-handed and one left-handed circularly polarized light line due to the red- or blueshift of absorption energy. Therefore, it is expected to observe one positive and one negative MCD peak around the absorption energy as shown in the case of  $B=4000$  or 5000 T or  $\text{Zn}_{1-x}\text{Cr}_x\text{Te}$  DMS.

#### IV. CONCLUSION

In this paper, we have calculated the MCD spectra of pure ZnTe within various magnetic field. The obtained MCD spectra in low magnetic field case are quite comparable with the experimental measurements and the magnitude is proportional to the magnetic field strength, consistent with the model understanding of MCD spectrum. When the magnetic field is very high and comparable with the SOC strength, it is found that the pure ZnTe has some similar band structures with those of Cr-doped ZnTe DMS. Accordingly, their MCD spectra also have similar structures around the two  $L$ -CPs. Such common MCD structure in pure and Cr-doped ZnTe DMS indicates that it is intrinsic and comes from the spin-split band structure of the host semiconductor. The differences in their MCD spectra are called extrinsic since they originate from the introduction of Cr 3d and 4s impurity bands. Therefore, we have demonstrated that the experimentally observed MCD spectra and its shape can be understood and well reproduced from the underlying band structures.

#### ACKNOWLEDGMENTS

The authors thank the staff of the Center for Computational Materials Science at IMR for their support and the use of Hitachi SR8000/64 supercomputing facilities. H. Weng acknowledges discussions with K. Ando and H. Saito and the hospitality while staying in RICS, AIST. X. Wan has contributed his critical reading and valuable comments on this paper.

\*Present address: Research Center for Integrated Science, Japan Advanced Institute of Science and Technology, Nomi, Ishikawa 923-1292, Japan. hmweng@jaist.ac.jp

<sup>1</sup>K. Ando, in *Magneto-Optics*, edited by S. Sugano and N. Kojima, Springer Series in Solid-State Science (Springer, Berlin, 2000), Vol. 128, Chap. 6.

<sup>2</sup>K. Ando, *Science* **312**, 1883 (2006).

<sup>3</sup>K. Ando, T. Hayashi, M. Tanaka, and A. Twardowski, *J. Appl.*

*Phys.* **83**, 6548 (1998).

<sup>4</sup>K. Ando, *Appl. Phys. Lett.* **82**, 100 (2003).

<sup>5</sup>H. Saito, W. Zaets, R. Akimoto, K. Ando, Y. Mishima, and M. Tanaka, *J. Appl. Phys.* **89**, 7392 (2001).

<sup>6</sup>K. Ando and H. Muneke, *J. Magn. Magn. Mater.* **272-276**, 2004 (2004).

<sup>7</sup>H. Saito, V. Zayets, S. Yamagata, and K. Ando, *Phys. Rev. Lett.* **90**, 207202 (2003).

- <sup>8</sup>K. Ando, H. Saito, Z. Jin, T. Fukumura, M. Kawasaki, Y. Matsumoto, and H. Koinuma, *Appl. Phys. Lett.* **78**, 2700 (2001); K. R. Kittilstved, W. K. Liu, and D. R. Gamelin, *Nat. Mater.* **5**, 291 (2006).
- <sup>9</sup>K. Ando, H. Saito, V. Zayets, and M. C. Debnath, *J. Phys.: Condens. Matter* **16**, S5541 (2004); K. Ando, arXiv:cond-mat/0208010 (unpublished).
- <sup>10</sup>H. Weng, J. Dong, T. Fukumura, M. Kawasaki, and Y. Kawazoe, *Phys. Rev. B* **73**, 121201(R) (2006).
- <sup>11</sup>H. Weng, J. Dong, T. Fukumura, M. Kawasaki, and Y. Kawazoe, *Phys. Rev. B* **74**, 115201 (2006).
- <sup>12</sup>H. Weng, Y. Kawazoe, and J. Dong, *Phys. Rev. B* **74**, 085205 (2006).
- <sup>13</sup>P. Blaha, K. Schwarz, G. K. H. Madsen, D. Kvasnicka, and J. Luitz, *WIEN2K: An Augmented Plane Wave+Local Orbitals Program for Calculating Crystal Properties* (Karlheinz Schwarz, Technische Universität, Wien, Austria, 2001).
- <sup>14</sup>J. P. Perdew, K. Burke, and M. Ernzerhof, *Phys. Rev. Lett.* **77**, 3865 (1996).
- <sup>15</sup>D. D. Koelling and B. N. Harmon, *J. Phys. C* **10**, 3107 (1977); A. H. MacDonald, W. E. Pickett, and D. D. Koelling, *ibid.* **13**, 2675 (1980).
- <sup>16</sup>H. Ebert, *Rep. Prog. Phys.* **59**, 1665 (1996).
- <sup>17</sup>J. Kuneš, P. Novák, M. Diviš, and P. M. Oppeneer, *Phys. Rev. B* **63**, 205111 (2001).
- <sup>18</sup>R. M. Dreizler and E. K. U. Gross, *Density Functional Theory, An Approach to the Quantum Many-Body Problem* (Springer-Verlag, Berlin, 1990).
- <sup>19</sup>T. Dietl, H. Ohno, F. Matsukura, J. Cibert, and D. Ferrand, *Science* **287**, 1019 (2002).
- <sup>20</sup>B. E. Larson, K. C. Hass, H. Ehrenreich, and A. E. Carlsson, *Phys. Rev. B* **37**, 4137 (1988); Małgorzata Wierzbowska, Daniel Sanchez-Portal, and Stefano Sanvito, *ibid.* **70**, 235209 (2004).
- <sup>21</sup>G. Theurich and N. A. Hill, *Phys. Rev. B* **66**, 115208 (2002).
- <sup>22</sup>A. K. Bhattacharjee, *Phys. Rev. B* **41**, 5696 (1990).
- <sup>23</sup>H. Saito, V. Zayets, S. Yamagata, and K. Ando, *J. Appl. Phys.* **93**, 6796 (2003).